

ATMOSPHERIC BOUNDARY LAYER FLOW OVER FOREST EDGES

ATMOSPHÄRISCHE GRENZSCHICHTSTRÖMUNG ÜBER WALDKANTEN

Ruck, B., Frank, C., Tischmacher, M.

Laboratory of Building- and Environmental Aerodynamics, Institute for Hydromechanics, Karlsruhe
Institute of Technology KIT, Kaiserstr. 12, 76128 Karlsruhe, Germany, e-mail: ruck@kit.edu

Key words: Wind field, forest edge, taper angle, flow over permeable edge

Schlagworte: Windfeld, Waldkante, Traufwinkel, Strömung über permeable Stufe

Abstract

The interaction of the atmospheric flow field with forest edges is of substantial interest for the storm stability of forest stands. In order to study the influence of the windward forest edge structure on the flow characteristics above the canopy, experimental investigations in an atmospheric boundary layer wind tunnel were carried out. Models of forest edges were exposed to a simulated atmospheric boundary layer flow. The taper angle of the edge was varied as well as the tree density of the stand. Time-averaged mean and turbulent flow quantities as well as spectral information were measured by means of a two-dimensional laser Doppler anemometer system (LDA).

Introduction

Woody plant ecosystems are strongly vulnerable to extreme events which are more and more associated with global climate change. As a consequence of this, researchers from climatology, biology, ecology and engineering are investigating adaptation strategies to strengthen the resistance and resilience of longevity woody plant ecosystems against storms heat, drought and flooding.

Considering storms, which contribute most to damages in forest stands reveals that devastating windthrow often starts from the edge region spreading into the stand. Of course, windthrow in forest stands depend on numerous parameters such as topography, tree density, canopy roughness, tree species, forest edge structure and soil parameters and windthrow can also occur directly inside a forest stand, i.e. far from any edge, triggered by downbursting gusts. However, the flow over the leading edge region of a forest induces strongest wind loads on trees. Near forest edges, the steepest gradients of velocity and pressure are found, giving rise to a higher probability of tree failure when compared to the inner stand. From a fluid mechanical point of view, forests represent a porous/permeable body in which turbulence can persist and forest edges are highly permeable steps (length of inner and outer forest edges in Germany is around 600.000 km), which strongly interact with the atmospheric boundary layer flow. Additionally, the canopy may have a longitudinal, lateral and vertical distribution of porosity. A detailed knowledge of the relations between these various influencing parameters and the flow field is necessary to work out silvicultural strategies for a future reduction of storm damage risk.

State of the art

Fundamental research in the field of flows and forests was carried out by Fritzsche 1933, Wölfle 1942 and Rottman 1986, who developed theories for the flow field behaviour at forest edges. Raynor 1971 carried out measurements of mean wind velocities at a forest edge. Ruck and Adams 1991 showed by wind tunnel simulation that the location of maximum turbulent shear stress is about 2-3 tree heights behind the leading edge, which is in good agreement with observations of e.g. Mitscherlich 1974. Kruijt et al. 1995 investigated in the field the progression of diffusive flow quantities in the edge region. Raupach et al. 1996 compared the flow over the canopy with a mixed-layer flow subject to Kelvin-Helmholtz instabilities. Irvine et al. 1997 measured the velocity field in the edge-near region and found that the internal boundary layer thickness is growing much slower than in the case above an impermeable wall. Finnigan 2000 gave an excellent review on turbulence in plant canopies. Morse et al. 2002 discussed the development of turbulence across a forest edge. Gardiner and Stacey 1996 and Dupont and Brunet 2008 investigated the influence of forest edge shape on stem bending moments. Li et al. 1990, Liu et al. 1996, Yang et al. 2006 and Frank and Ruck 2008 carried out numerical computations simulating momentum fluxes over the forest edge.

Despite the fact that the forest edge has been the center of interest in many studies, it is up to now not clear, how stand density and forest edge structure alter the flow field situation at the canopy-near forest edges in detail. This is due to the fact that field measurements cannot provide the required variation of stand structure for a systematic investigation of the problem and that numerical simulations are presently not able to describe individual tree aerodynamics. To contribute to the knowledge of interaction of wind field and forest edges, detailed flow field investigations near the canopy were performed. Edge shape and stand density were varied in these investigations.

Forest models

For the wind tunnel investigations, forest models were used consisting of rigid model firs to obtain a good geometrical similarity with real coniferous trees. The scale of the models was 1:200. As the reference case, the most dense configuration was used, in which the model forest was made of 6700 single trees and the distance between model trees in main flow direction x was $a_x = 2.06\text{cm}$ (4.1m) and in lateral y -direction almost equal, i.e. $a_y = 2.00\text{cm}$ (4.0 m). The reference case will be denoted as (BD100). The forest model extended over a length of 2.06m in x -direction and nearly all of the wind tunnel width of 1.5m. This resulted in a stand density of 2400 trees per square meter for the model and 600 trees per hectare in nature respectively. The mean height H of a single tree and thus the height of the canopy top was 11.5cm which corresponds to 23m in nature. These values fit very well with statistical data published by the National Forest Inventory of Germany 2002. The height of single trees showed a natural variability in the range of 0.5cm, i.e. 1m in nature. The stems, on which model fir crowns of 2.5cm width and 6cm height have been mounted, were polystyrene-rods of 4mm diameter and a mean height of $S = 5.5\text{cm} = 0.48H$. By removing whole rows of the originally dense model forest, see Fig. 1, the density of the homogenous forest stands was varied. The arrangement where every second row was removed is denoted as BD50 and the one where every second to fourth row was removed is denoted as BD25.

The structure of the leading forest edge was varied in the experiments. Two types of edge models were used, homogeneous edges made of highly porous foam as well as edges consisting of single model trees. For the latter, first the stem height was diminished and for trees less high than $K=6\text{cm}$, the top of the crown was cut. The individual trees were arranged at distances of 2cm x 2cm. In the former case the used foam material was characterized by a

very uniform, open-celled structure specified by 10 p.p.i (i.e. 10 pores per inch, cell size = ca. 2.5 mm) and a pore volume fraction of 97%. The pressure loss coefficient of this foam amounted in model scale to $kr,M = 300 \text{ m}^{-1}$ corresponding to $kr,N = 1.5\text{m}^{-1}$ in full scale.

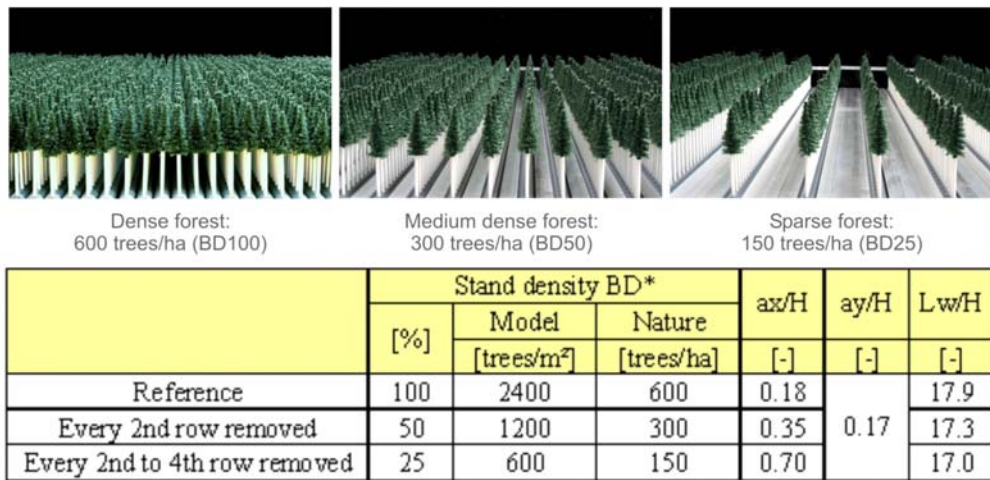


Figure 1: Homogenous forest stands: outline of tests; ax = spacing between the trees in stream-wise direction, ay = spacing between the trees in lateral direction (perpendicular to the approach flow), Lw = length of the forest = distance between first and last tree row, H = mean stand height = 23 m, *stand density based on the ground area of the reference configuration

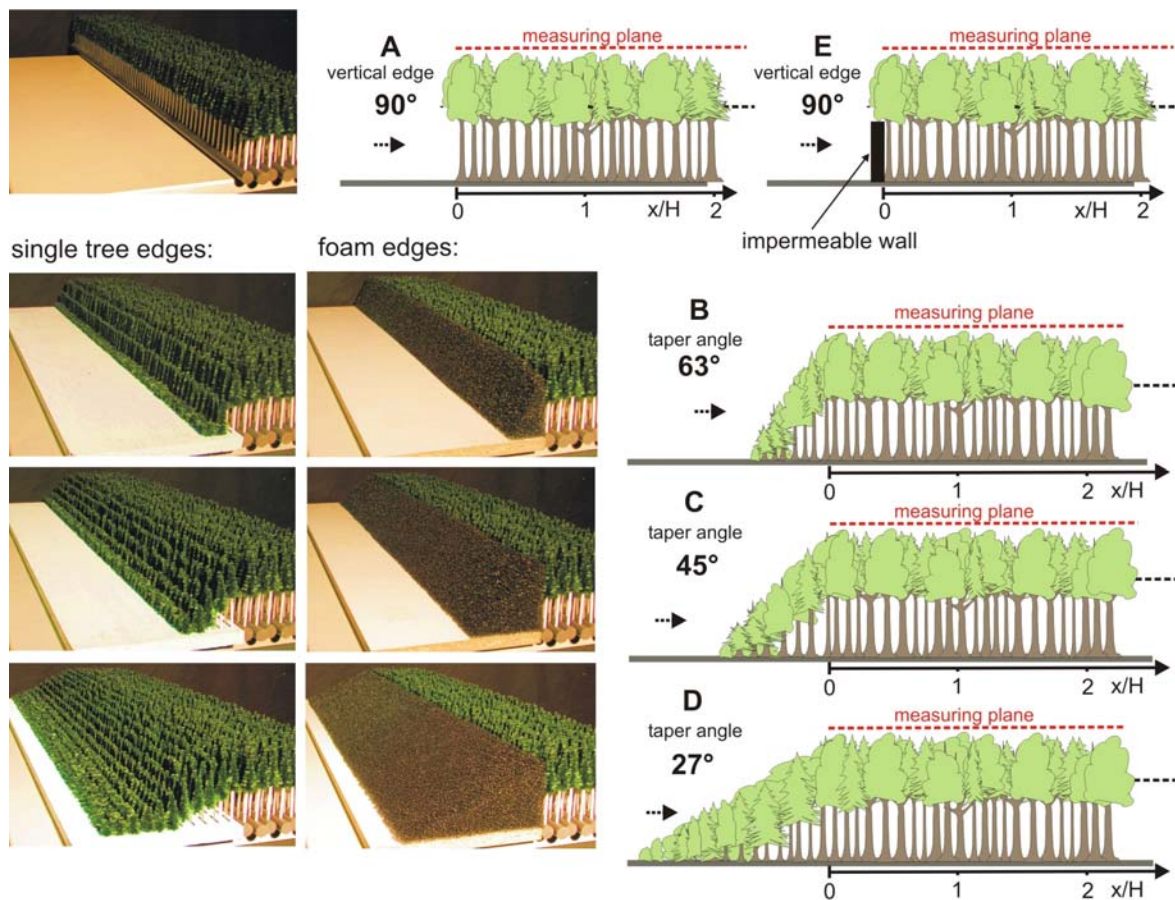


Figure 2: Forest models with different edge structures: A) forest edge with open trunk space; B), C), D) single tree edges with taper angles $TW=63^\circ, 45^\circ, 27^\circ$, E) figure of dense forest with impermeable wall

The height of the foam edges amounted to 11cm at the windward stand edge, thus, the edge was slightly lower than the mean stand height $H = 11.5\text{cm}$. The structure of the single tree edges is less uniform, but more natural and slightly sparser than that of the foam edges. The taper angle TW of the edges was varied three times for both edge types.

For the investigations, the different edges were combined with both, the dense stand (BD100) and the sparse stand (BD25), where every 2nd to 4th row was removed (see also Frank and Ruck, 2009). In addition, a configuration was investigated where the airflow in the trunk space of the dense forest was blocked completely by the windward arrangement of an impermeable wall (Fig. 2)

Flow analysis

The velocity measurements were accomplished by means of a two-component laser Doppler anemometer (2D-LDA) system. At every measuring point, about 26 600 data points were sampled in coincidence mode with a sampling frequency of 500 Hz. Hence, one point measurement took 53 s. The main flow direction was perpendicular to the stand edge. The origin of the used x,z -coordinate system is located on the wind tunnel floor at the windward side of the actual stand (i.e. at the leeward side of the upstream forest edges) with the x -axis in horizontal streamwise direction and the z -axis in upward oriented vertical direction.

From the measured instantaneous velocities $U(x,z,t)$ in main flow direction and $W(x,z,t)$ in vertical direction the mean velocities $u(x,z)$, $w(x,z)$ and therefrom the turbulent fluctuations $u'(x,z,t)$, $w'(x,z,t)$ using the decompositions $U=u+u'$ and $W=w+w'$ were computed. Further, the mean vertical momentum flux $\overline{u'w'}$ was derived. A negative value of $\overline{u'w'}$ tells that the flux is directed downwards and the magnitude gives a measure for its strength. Hence, this term is of high interest, as it is a widespread assumption that downward flowing gusts are at least partly responsible for windthrow and windbreak. For more detail on this issue, the momentum flux above homogeneous stands with respect to its fractions of sweeps ($u'>0$, $w'<0$), bursts ($u'<0$, $w'>0$), outward and inward interactions ($u'>0$, $w'>0$ and $u'<0$, $w'<0$ respectively) was analysed. In order to detect the flow phenomena near the canopy top, measurements were carried out at a height as close as technically possible over the canopy top, i.e. $z/H = 1.13$, and with a high spatial resolution between $1\text{ cm} = 0.087 \cdot H$ (2 m in nature) near the windward edge and $5\text{ cm} = 0.435 \cdot H$ (10 m) near the leeward edge.

The simulated Atmospheric Boundary Layer

To simulate real atmospheric flow processes in the wind tunnel, a simulation of an atmospheric boundary layer is required, see Counihan 1975. Since the main focus was on strong wind conditions, a neutrally stratified atmospheric boundary layer was simulated. A neutral boundary layer can be characterized adequately by the mean wind velocity profiles, turbulence profiles and the energy distribution of the gusts (Plate 1995). To generate an appropriate approach wind profile, spires and roughness elements were used, see Frank and Ruck (2007). Figure 3 shows good agreement between the simulated boundary layer and literature data (Eurocode 1:2005, Plate 1995) for an approaching flow over suburban terrain ($\alpha = 0.26$, $z_0=1.9\text{ mm}$ i.e. 0.38 m in natural scale).

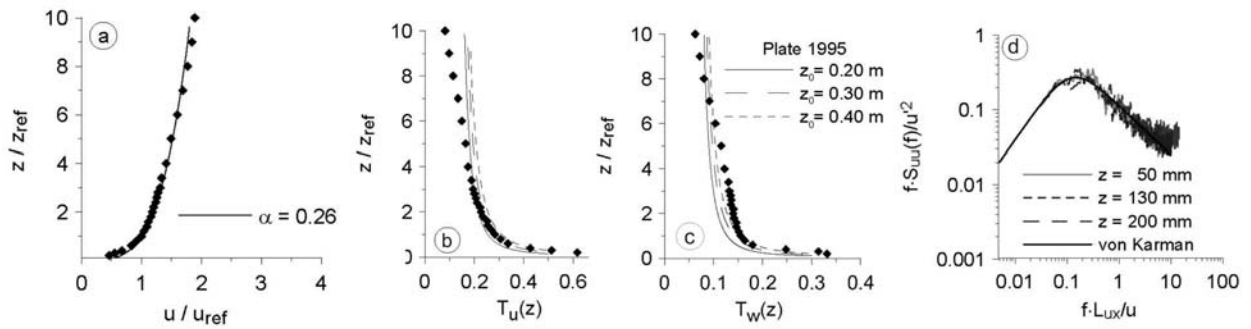


Figure 3: Simulated atmospheric boundary layer: a) time-averaged horizontal velocity $u(z)$ ($z_{\text{ref}} = 0.05 \text{ m}$, $u_{\text{ref}} = 4.34 \text{ m/s}$), b) turbulence intensity in main flow direction $T_u(z)$, c) Turbulence intensity in vertical direction $T_w(z)$, d) Normalized spectral density functions $f \cdot S_{uu}(f)/u^2$

In Fig. 3d, dimensionless spectral density functions measured at three different heights are shown together with the von Kármán spectrum. The spectra match very well in terms of location and height of the maximum and almost two decades of the inertial range are resolved. This indicates that the behaviour of the large scales, which carry the greatest part of the kinetic energy in the flow, were correctly resolved.

Results

First of all, a most interesting question is how the flow develops over the edge in vertical wind direction. Fig. 4 gives the angle of the mean flow directly above the canopy in the x - z -plane along the dashed measuring line. As can be seen, the flow angle starts between 12° - 15° depending on the taper angle of the edge and decreases with distance from the edge. This shows that in time-mean consideration at the edge region, there is a vertical outflow of mass through the canopy in upward direction, which decreases with x/H . The time-mean vertical outflow mass flux is caused by a time-mean horizontal inflow mass flux at the windward edge of the forest. It can also be inferred that a smaller taper angle of the edge, which is equivalent to longer edge shapes, slows down the approaching wind more effectively, so that the frontal inflow mass flux into the canopy and trunk space is reduced. As a consequence, this leads to smaller angles of the time-mean outflow, i.e. to a smaller vertical outflow mass flux.

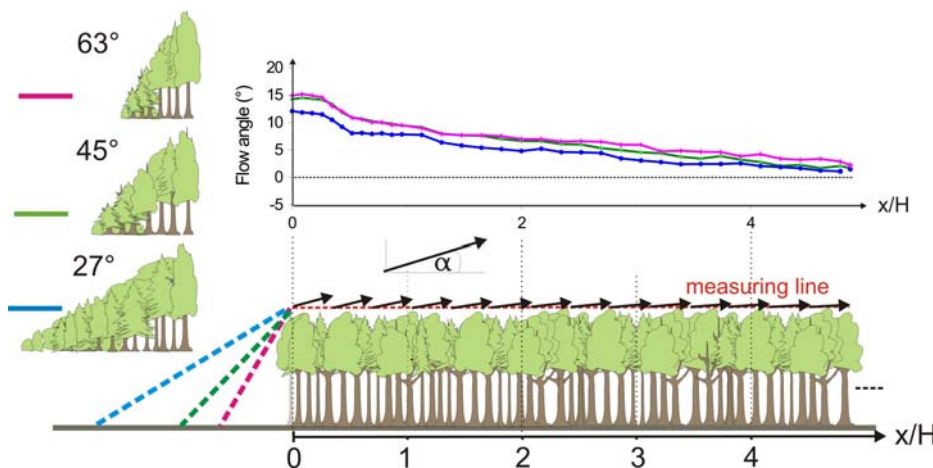


Fig. 4: Flow angle of the time-mean outflow through the canopy, measured at $z/H=1.13$; tapered edges consisting of single trees, tree density BD100, taper angle 27° , 45° , 63°

From the time-mean results shown in Fig. 4 it cannot be concluded that there is a continuous outflow through the canopy. Instead, instantaneous gusts penetrate into the canopy and lead to instantaneous wind loading. To describe this gust flux, the turbulent momentum flux can be measured indicating the x -momentum flux transported in z -direction, see Fig. 5.

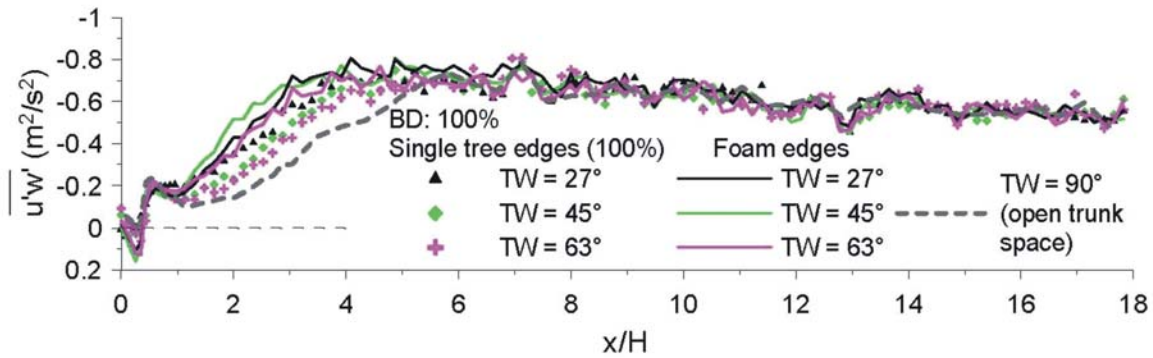


Fig. 5 Dependency of time-averaged turbulent momentum flux $\overline{u'w'}$ close to the canopy top ($z/H = 1.13$) above a dense stand (BD100) on different windward forest edges

As can be seen from Fig. 5, the turbulent momentum flux $\overline{u'w'}$ increases and reaches its peak value between $4 < x/H < 8$, depending on the edge angle. The results agree well with former studies, see Ruck and Adams (1991). The curves for smaller edge angles are shifted a little towards the upstream forest edge indicating that the turbulent momentum exchange is increasing earlier due to the longer way over a forested canopy. A more detailed picture of the vertical momentum flux can be obtained by quadrant analysis, see Shaw et al. 1983. With this analysis, the sign of u' and w' forming a time series of $u'w'(t)$ is analyzed. The products $u'w'(t)$ are sorted in 4 quadrants according to the individual sign of its components. Quadrant 1 contains all values of $(+u')*(+w')$, quadrant 2 all values of $(-u')*(+w')$, quadrant 3 all values of $(-u')*(-w')$ and quadrant 4 all values of $(+u')*(-w')$. Using these criteria, one can subdivide into downward momentum flux (quadrant 2 and 4) and upward momentum flux (quadrant 1 and 3). Using bivariate histograms, the joint probability distributions from simultaneously measured values of u' and w' can be displayed indicating probabilities of occurrence of certain combinations, see Fig. 6.

Considering the spectra of velocity fluctuations in the horizontal streamwise direction at different positions A – H, see Fig. 7, reveals that the turbulence of the approaching flow (position A) is on a moderate level (the area under each curve is proportional to the variance of the fluctuations). The spectrum alters with distance from the edge. As can be seen at position B and C, turbulence is produced in the range of higher frequencies. This phenomenon is mainly due to the generation of wake turbulence behind individual tree components like needles, branches, stems and whole crowns. Especially, in the region, where strong horizontal momentum can be transported vertically, the generation of wake turbulence is on a high level. After rebuilding a new internal boundary layer, far behind the edge, the production of mean wind wake turbulence is decreasing and the drag in the canopy is sustained mainly by vertical turbulent mixing. Nevertheless, the area beneath the curves is greater than in the approach flow, underlining that the turbulence remains on a high level near the rough canopy. It seems that smaller taper angles induce in the edge-near region slightly higher turbulence levels. Another most interesting aspect is the skewness of the wind velocity distribution near the canopy at the edge region, see Fig. 8. As can be seen, the skewness is positive near the edge and tends to nil inside the forest far from the edge. This means that the span of the velocity fluctuations right from the mean is greater than left from the mean suggesting that strong wind velocities may occur. Inside the stand, the distribution becomes symmetrical indicating that fluctuation velocities above and below the mean are equally distributed.

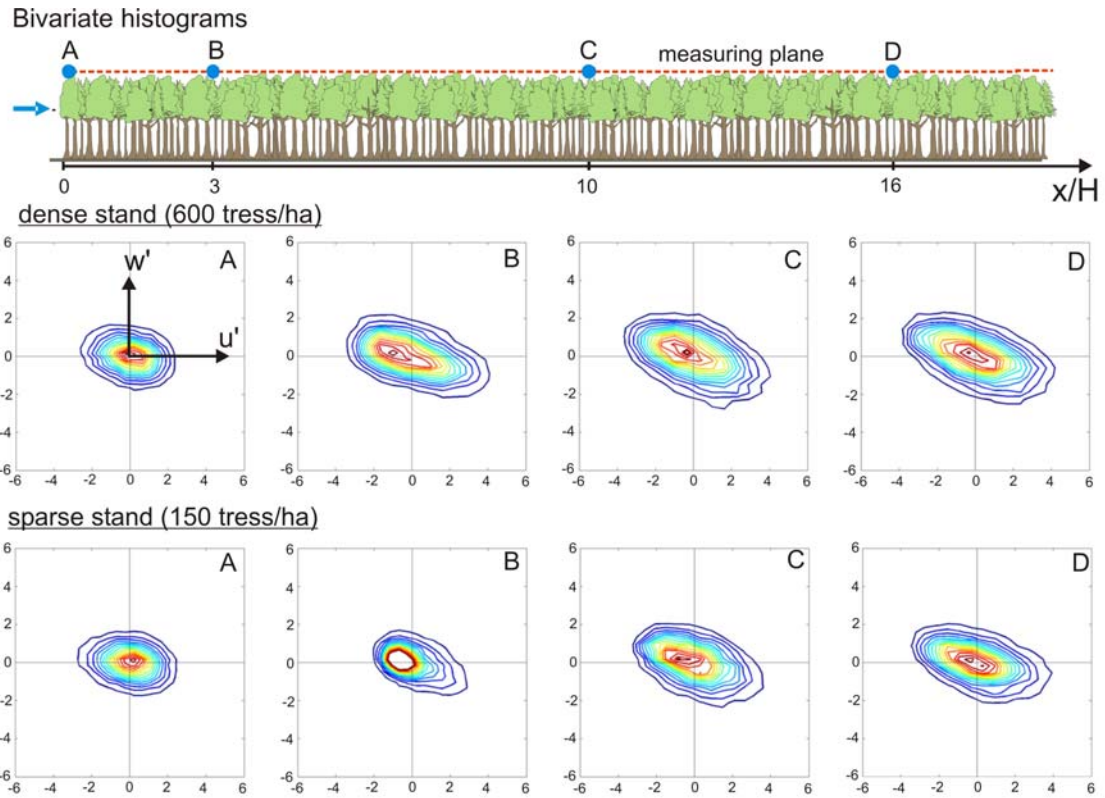


Fig. 6: Bivariate histograms of joint probability distributions of u' and w' at four positions A, B, C, D

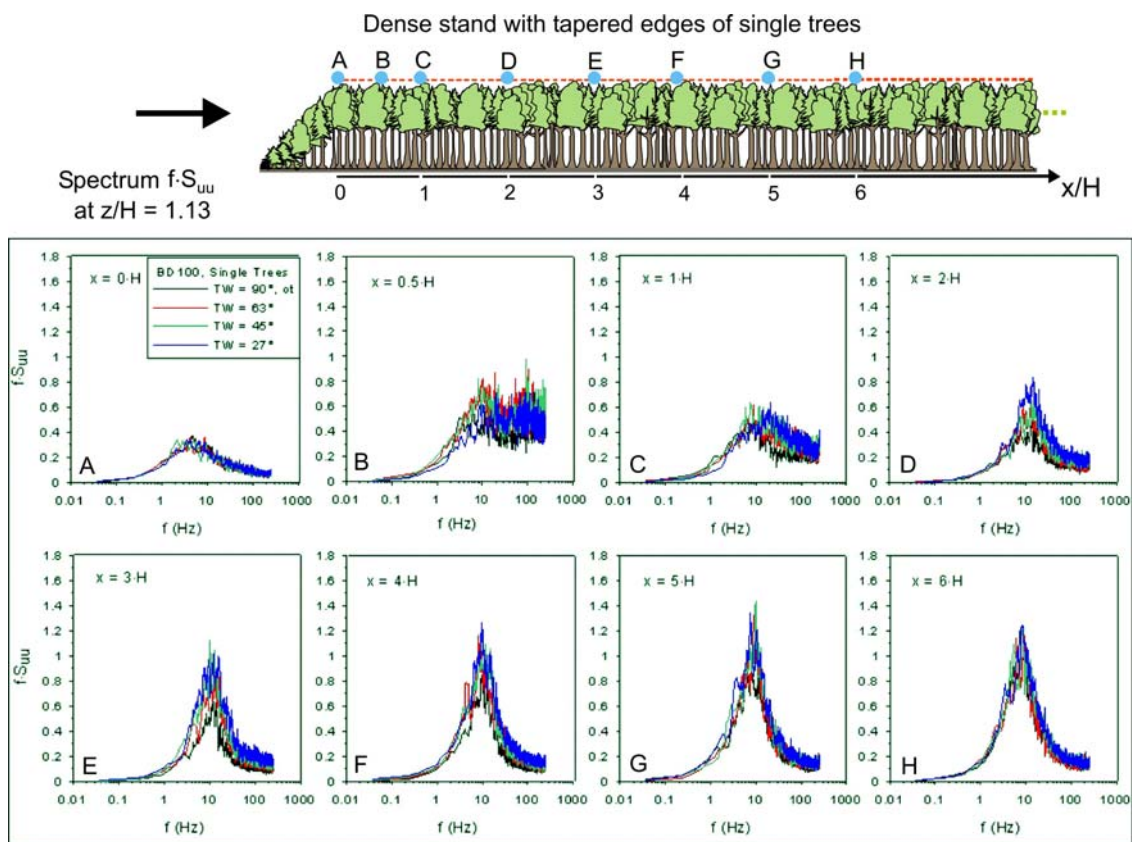


Fig. 7: Spectrum of horizontal streamwise wind fluctuations close to the canopy of a dense forest with tapered edges, tree density BD100, taper angle 27° , 45° , 63° , 90°

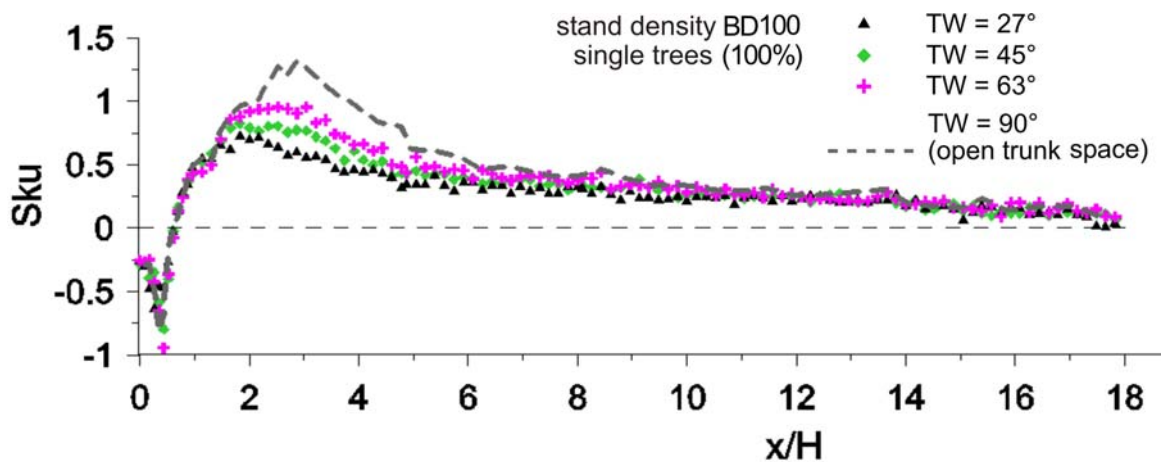


Fig. 8: Skewness of the velocity distribution near the canopy ($z/H=1.13$) at the edge region for a dense forest (BD100 = 600 trees/ha), taper angle 27°, 45°, 63°, 90°

Conclusion

Resuming the results of this study and former studies allows to set-up a sketch, which comprises the main features of the flow across a forest edge, see Fig. 9. The atmospheric flow interacts with the forest edge as follows: At the leading edge the oncoming flow is partially blocked and displaced. As a consequence of this, a region of overpressure forms before the edge decaying into the forest. A part of the flow enters the branch-free stem volume and is decelerated.

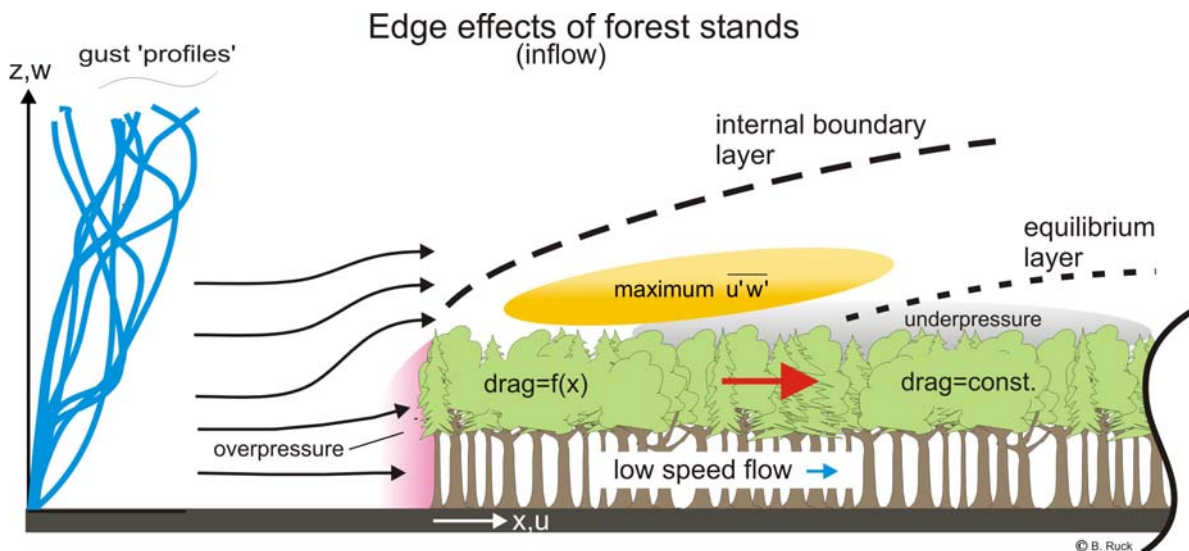


Fig. 9: Main features of the flow across a forest edge

A second part of the oncoming flow (and momentum) enters the crown volume and is slowed down very quickly in the porous canopy. Thus, the edge-near trees have to bear the highest wind loads due to drag induced by pressure and friction. A third part of the approaching atmospheric flow is displaced and flows over the canopy. A new internal boundary layer builds up showing highest canopy-near velocities at the beginning (edge). This leads to highest friction values at the edge-near canopy top. Furthermore, the flow over the canopy resembles a mixing-layer flow where two layers of different wind velocity (crown layer and above-canopy layer) meet at an interface giving rise to vortical instabilities (Kelvin-Helmholtz instability \rightarrow coherent structures). However, this mixing-layer flow is particular, since the differen-

tial velocity between the layers is not constant, but decrease starting from the edge. This leads to a region of highest exchange of vertical momentum, which is found in a distance of $4 < x/H < 8$ behind the edge. The above explanations refer mainly to mean flow and statistical turbulent quantities. In reality, there is a dynamic coupling between wind field and tree/crown movement (wind loads). Thus, fluid-structure interactions caused by individual gusts have to be considered in tree failure analyses.

Acknowledgement

The investigations shown were performed within two projects a) 'Improving the storm stability of forest stands' which is part of the RESTER-network ('Strategies for the reduction of the storm damage risk for forests') within the research program 'Challenge climate change', b) "The highly unsteady interaction of gusts and forest edges", DFG-grant No. Ru 345/30. The authors would like to thank the Ministry for the Environment of the German federal state Baden-Württemberg and the Deutsche Forschungsgemeinschaft DFG for the financial support.

Literatur

- Counihan, J., 1975:** "Adiabatic Atmospheric Boundary Layers: A Review and Analysis of Data from the Period 1880-1972", Atmos. Environ. 9, 871-905, Pergamon Press.
- Dupont, S., Brunet, Y., 2008:** 'Impact of Forest Edge Shape on Tree Stability: A Large-Eddy Simulation Study', Forestry 81(3), 299-316.
- Eurocode 1: 2005:** Einwirkungen auf Tragwerke – Teil 1-4: Allgemeine Einwirkungen, Windlasten; Deutsche Fassung EN 1991-1-4:2005
- Finnigan, J., 2000:** 'Turbulence in Plant Canopies', Annu. Rev. Fluid Mech., 32, 519-571
- Frank, C., Ruck, B., 2007:** „Windkanalstudie zur Strömung in Waldlichtungen“, Proc. 15. Fachtagung Lasermethoden in der Strömungsmesstechnik, Rostock, 9.1-9.9.
- Frank, C., Ruck, B., 2008:** "Numerical Study of the Airflow over Forest Clearings", 2008, Forestry 81(3), 259-277
- Frank, C., Ruck, B., 2009:** "About the influence of the stand density on the flow characteristics at forest edges", Proc. 2nd Int. Conf. on Wind Effects on Trees, University of Freiburg
- Fritzsche, K., 1933:** Sturmgefahr und Anpassung. Tharandter Forstliches Jahrbuch, 84:1-94
- Gardiner, B., Stacey, G., 1996:** 'Designing Forest Edges to Improve Wind Stability', Forestry Commission, Technical Paper 16, 8 pages
- Irvine, M.R., Gardiner, B.A., Hill M.K., 1997:** 'The evolution of turbulence across a forest edge'. Boundary Layer Meteorology, 84:467-496
- Kruijt, B., Klaassen, W., Hutjes, R.W.A., 1995:** 'Edge Effects on Diffusivity in the Roughness Layer over a Forest'. In: Coultis and Grace (eds.), Proc. of the IUFRO Conference on Wind and Wind Related Damages to Trees, Edinburgh, pp 60-70, Cambridge University Press
- Li, Z., Lin, J.D., Miller, D.R., 1990:** 'Air Flow Over and Through a Forest Edge: A Steady-State Numerical Simulation', Boundary Layer Meteorology 51:179-197
- Liu, J., Chen, J.M., Black, T.A., Novak, M.D., 1996:** 'Modelling of turbulent air flow downwind of a model forest edge'. Boundary Layer Meteorology, 77:21-44
- Mitscherlich, G., 1974:** „Sturmgefahr und Sturmsicherung“. Schweizerische Zeitschrift Forstwesen, 125:199-216
- Morse, A.P., Gardiner, B.A., Marshall, B.J., 2002:** 'Mechanisms controlling turbulence development across a forest edge'. Boundary Layer Meteorology, 103:227-251
- Plate, E.J., 1995:** „Windprofile in der Gebäudeaerodynamik. In: Plate, E.J. (ed.) Windprobleme in dichtbesiedelten Gebieten, WTG-Berichte Nr. 3, 7-26, Windtechnologische Gesellschaft, Aachen
- Raupach, M.R., Finnigan, J.J., Brunet, Y., 1996:** 'Coherent eddies and turbulence in vegetation canopies: the mixing-layer analogy', Boundary-Layer Meteorology 78, 351-382
- Raynor, G.S., 1971:** 'Wind and temperature structure in a coniferous forest and a contiguous field', Forest Science, 17:351-363
- Rottmann, M., 1986:** „Wind- und Sturmschäden im Wald“, Beiträge zur Beurteilung der Bruchgefährdung, zur Schadensvorbeugung und zur Behandlung sturmgeschädigter Nadelholzbestände, J.D. Sauerländer's Verlag, Frankfurt am Main, 128 S.
- Ruck, B., Adams, E., 1991:** "Fluid Mechanical Aspects in the Pollutants Transport to Coniferous Trees", Boundary Layer Meteorology, 56, 163-195
- Shaw, R.H., Tavangar, J., Ward, D.P. 1983:** 'Structure of the reynolds stress in a canopy layer', Journal of Climate and Applied Meteorology, 22:1922-1931
- Wölfle, M., 1942:** „Windverhältnisse im Walde“, III. Einfluß von Unter- und Zwischenstand auf die Windverhältnisse über der Bestandsrandzone. Forstw. Centralblatt 64, 8:169-182
- Yang, B., Shaw, R.H., Paw U, K.T., 2006:** 'Wind loading on trees across a forest edge: A large eddy simulation'. Agric. Forest Meteorol., 141:133-146